HHS Public Access

Author manuscript

Acta Biomater. Author manuscript; available in PMC 2016 June 01.

Published in final edited form as:

Acta Biomater. 2015 June ; 19: 23–32. doi:10.1016/j.actbio.2015.03.012.

Biphasic silica/apatite co-mineralized collagen scaffolds stimulate osteogenesis and inhibit RANKL-mediated osteoclastogenesis

Jiao Kai[1,#], **Li-na Niu**[1,#], **Qi-hong Li**[2,#], **Fa-ming Chen**[1], **Wei Zhao**[3], **Jun-jie Li**[3], **Ji-hua Chen**[1,*], **Christopher W Cutler**[4], **David H Pashley**[4], and **Franklin R Tay**[4,*]

[1]State Key Laboratory of Military Stomatology, School of Stomatology, The Fourth Military Medical University, Xi'an, China

[2]Department of Stomatology, Affiliated Hospital of Academy of Military Medical Science, Beijing, China

[3]Xijing Hospital, The Fourth Military Medical University, Xi'an, China

[4]College of Dental Medicine, Georgia Reagents University, Augusta, GA, USA

Abstract

The effects of a biphasic mineralized collagen scaffold (BCS) containing intrafibrillar silica and apatite on osteogenesis of mouse mesenchymal stem cells (mMSCs) and inhibition of receptor activator of nuclear factor κB ligand (RANKL)-mediated osteoclastogenesis were investigated in the present study. mMSCs were cultured by exposing to BCS for 7 days for cell proliferation/viability examination, and stimulated to differentiate in osteogenic medium for 7–21 days for evaluation of alkaline phosphatase activity, secretion of osteogenic deposits and expression of osteoblast lineage-specific phenotypic markers. The effect of BCS-conditioned mMSCs on osteoclastogenesis of RAW 264.7 cells was evaluated by tartrate-resistant acid phosphatase staining and resorption pit analysis. The contributions of mitogen-activated protein kinase (MAPK) and phosphatidylinositol-3 kinase (PI3K) signal transduction pathways to osteogenesis of mMSCs and their osteoprotegerin (OPG) and RANKL expressions were also evaluated. Compared with unmineralized, intrafibrillarly-silicified or intrafibrillarly-calcified collagen scaffolds, BCS enhanced osteogenic differentiation of mMSCs by activation of the extracellular signal regulated kinases (ERK)/MAPK and p38/MAPK signaling pathways. After mMSCs were exposed to BCS, they up-regulated OPG expression and down-regulated RANKL expression through activation of the p38/MAPK and PI3K/ protein kinase B (Akt) pathways, resulting in inhibition of the differentiation of RAW 264.7 cells into multinucleated osteoclasts and reduction

[*]**Co-corresponding authors: Dr. Franklin Tay:** Department of Endodontics, College of Dental Medicine, Georgia Reagents University, Augusta, GA, USA; ftay@gru.edu; Tel.: +1 706 721 2033; Fax: +1 706 721 6252; **Dr. Ji-hua Chen:** State Key Laboratory of Military Stomatology, School of Stomatology, Fourth Military Medical University, Xi'an, China; jhchen@fmmu.edu.cn; Tel.: +86 029 84776001.

[#]These authors contributed equally to this work

in osteoclast function. These observations collectively suggest that BCS has the potential to be used in bone tissue engineering when the demand for anabolic activities is higher than catabolic metabolism during the initial stage of wound rehabilitation.

Keywords

intrafibrillar mineralization; hydroxyapatite; osteogenesis; osteoprotegerin; osteoclastogenesis; silica

1. Introduction

Nature's paradox of achieving complexities in structural design via the use of simplistic motifs has inspired scientists to investigate the mechanisms responsible for collagen biomineralization, and to mimic those mechanisms for the design of bioinspired materials for treatment of mineralization-related diseases [1–3]. Recent advancements in the understanding of the mechanistic aspects of collagen biomineralization contributed to the production of three-dimensional calcified collagen scaffolds that are based on highly-ordered deposition of apatite crystallites within the intrafibrillar compartments of fibrillar collagen. These apatite-containing scaffolds were produced using poly(acid) biomimetic analogs of matrix non-collagenous proteins for stabilizing amorphous calcium phosphate [4–7]. However, these calcified collagen scaffolds (CCS) are only osteoconductive since apatite crystallites exert negligible anabolic (bone-forming) effects on mesenchymal stem cells [8,9]. In addition, CCS are not perfect for bone tissue engineering because of their brittleness, low degradability and their limited capability to influence the catabolic (bone-resorbing) activities of bone metabolism.

Intrafibrillar silicification of collagen was developed by harnessing the essence of biomineralization principles involved in the formation of diatom frustules [10]. Such a procedure produces 3-D silicified collagen scaffolds (SCS) containing deposition of poly(amine)-stabilized orthosilicic acid that subsequently condensed into a highly-ordered arrangement of intrafibrillar amorphous silica nanoparticles [11]. The rationale for producing SCS was based on the premise that silicic acid/silica has the potential to influence both the anabolic and catabolic aspects of bone metabolism [12]. Silica components, such as orthosilicic acid, biosilica and silica nanoparticles, stimulate type I collagen synthesis and osteoblast differentiation in human osteoblast-like cells *in vitro* [13,14]. These stimulatory effects on osteoblasts has been reported to be regulated by phosphorylation of extracellular signal regulated kinases (ERK), p38 kinases (p38) and protein kinase B (Akt kinases) [15,16]. Silica nanoparticles also inhibit osteoclast differentiation *in vitro* [17]. These effects are the consequence of silicon's intrinsic capacity to modulate the expression of receptor activator of nuclear factor κB ligand (RANKL)/osteoprotegerin (OPG) [17], the latter plays an important role in modulating the cross-talk between osteoblasts and osteoclasts [18]. RANKL inhibits osteoblastic bone formation but is necessary for differentiation of osteoclasts [17]. Osteoprotegerin acts as a decoy receptor that binds to RANKL and prevents it from binding to the RANK expressed by hematopoietic precursor cells, thereby inhibiting differentiation of osteoclast precursors into mature, multinucleated osteoclasts [19].

Signaling pathways regulating the expression of RANKL and OPG have been reported previously; phosphorylation of ERK, p38 are involved in RANKL expression by osteoblastic cells, while phosphorylation of p38 and Akt kinases are involved in OPG expression [20,21].

Silicified collagen scaffolds have been shown to be biodegradable, osteoinductive and angiogenic, due to their ability to up-regulate expressions of osteogenesis-related genes of mesenchymal stem cells and angiogenesis-related genes of endothelial progenitor cells [22]. However, their compressive strength (tagent modulus: 574.5 KPa and modulus of toughness: 137.3 KPa) is lower than that of CCS (9.97 MPa and 1.63 MPa, respectively) due to the amorphous nature of intrafibrillar silica [11,23], which requires temperatures much higher than the combustion temperature of collagen to attain crystallinity. To combine the advantages of SCS and CCS, a hybrid biomineralization scheme was developed by the authors that resulted in intrafibrillar mineralization of collagen fibrils with ordered arrangement of silica-apatite biphasic minerals [23]. The mineralization mechanism involves infiltration of poly(acid)-stabilized calcium phosphate precursors within the intrafibrillar spaces of the SCS, which results in the growth of apatite crystallites within the partially-silicified collagen fibril. This hybrid mineralization strategy generated a biphasic mineralized collagen scaffold (BCS) with increased resilience and fatigue resistance, due to the interpenetrating arrangement of amorphous silica, collagen molecules and crystalline apatite [23]. The tangent modulus and modulus of toughness of the BCS are 8.26 MPa and 2.05 MPa, respectively. Although the BCS is not as stiff as CCS, it is tougher and has a higher capacity to absorb energy when subjected to compressive stress in the bone defects [23]. The resilience of BCS enables it to be compressed during insertion into a bony defect and expand to adapt to the conformation of the defect. Moreover, because of the presence of biphasic mineral components in BCS, it is anticipated that BCS may possess dual anabolic and anti-catabolic effects when they are seeded with mesenchymal stem cells. Hence, the objective of the present study was to compare the effects of BCS with other mineralized scaffolds (CCS and SCS) on the osteogenesis and osteoclastogenesis inhibitory effects of mesenchymal stem cells (MSCs), and to determine the signal transduction pathways in the MSCs which are responsible for those potential effects. The null hypotheses tested were: 1) there is no difference among the unmineralized and mineralized collagen scaffolds with different intrafibrillar minerals in stimulating osteogenesis of mMSCs; and 2) there is no difference among the various collagen scaffolds in their indirect inhibition of RANKL-mediated osteoclastogenesis and osteoclast function.

2. Materials and methods

2.1 Preparation of SCS, CCS and BCS

Silicified, calcified and biphasic mineralized collagen scaffolds were prepared as described previously [5,10,23]. Briefly, collagen scaffolds (CS, 5-mm diameter, 2-mm thick) were punched from reconstituted type I collagen tapes (Ace Surgical Supply Co. Inc., MA, USA). Silicified collagen scaffold (SCS) were prepared by incubating CS for 2 days in a silicifying medium consisting of 5% silicic acid that was stabilized with poly(allylamine) hydrochloride (PAH, Mw 15,000; Sigma-Aldrich, St. Louis, MO, USA). Calcified collagen

scaffolds (CCS) were prepared by incubating CS in calcifying medium (4.5 mM $CaCl_2 \cdot 2H_2O$, 2.1mM K_2HPO_4 and 50-μg/mL Poly-L-aspartic acid in Tris-buffered saline) at 37 °C for 14 days. For the preparation of biphasic mineralized collagen scaffolds (BCS), the CS were first immersed in silicifying medium at 37 °C for 2 days and further incubated in calcifying medium for 7 days.

The status of intrafibrillar mineralization of the SCS, CCS and BCS were examined with transmission electron microscopy (TEM). Briefly, mineralized specimens were fixed in 2% glutaraldehyde, dehydrated in an ascending ethanol series (50–100%), immersed in propylene oxide and embedded in epoxy resin. Ninety nanometer thick sections were examined without further staining using a JSM-1230 TEM (JEOL, Tokyo, Japan) at 110 kV. Selected area electron diffraction (SAED) was performed to identify the crystallinity of the infiltrated minerals.

2.2 Release of silicic acid and calcium ions from BCS

Cumulative release of silicic acid from SCS and BCS was examined with the silicomolybdic acid spectrophotometric method [29].Ten dried SCS and BCS were immersed in 15 mL of Tris-buffered saline (TBS; pH 7.4), respectively. At designated time periods (1–7 days), 400 μL aliquots of the orthosilicic acid-containing TBS were withdrawn from the respective solutions and added to deionized water (4.6 mL). With continuous stirring, 2.5 mL of 1.0 N HCl, 2.5 mL of Na_2EDTA (26.9 mM), and 2.5 mL of ammonium molybdate solution (42.1 mM; pH 8) were added to the orthosilicic acid-containing TBS solutions. After 5 min, 2.5 mL of tartaric acid (0.67 M) was added to the solutions, followed by the addition of 5 mL of sodium sulfite (1.35 M). Absorbance of the solutions was recorded after 30 min using a spectrophotometer (Synergy HT, BioTek Instruments, Winooski, VT, USA) at $\lambda = 700$ nm.

For detection of calcium ion release, ten dried CCS and BCS were immersed in 15 mL of TBS respectively. At designated time periods (1–7 days), the cumulative release of calcium ions was measured using a calcium ion electrode.

2.3 Cells and incubation conditions

Mouse mesenchymal stem cells (mMSCs; C57Bl/6-TgN(ACTbEGFP)1Osb, Texas A&M Health Science Center, Institute for Regenerative Medicine, College Station, TX, USA) or murine macrophage-like RAW 264.7 cells (ATCC, Manassas, VA, USA) were cultured in α-MEM medium containing 10% fetal bovine serum and 100 U/mL penicillin/streptomycin. Cells from the third to sixth passages were used for cell proliferation, osteogenesis or osteoclastogenesis studies. The CS, SCS, CCS and BCS disks (5-mm diameter, 2-mm thick) were rinsed thoroughly with deionized water, sterilized using gamma-radiation at 25 kGy and incubated in the culture medium for 24 hr prior to further experiments.

2.4 Cell proliferation and viability assays

2.4.1 DNA content quantification—To study cell proliferation on the scaffolds, 1×10^4 mMSCs were seeded onto CS, SCS, CCS and BCS disks (N=6) and cultured in 1.5 mL of culture medium for one week. The cells were digested with proteinase K overnight at 56 °C. The DNA concentration was determined using PicoGreen™ DNA assay (Invitrogen, Life

Technologies, Grand Island, NY, USA) at an excitation wavelength of 480 nm and emission wavelength of 530 nm, using a calibration curve of lambda DNA standards. Experiments were conducted in sextuplicates (N=6).

2.4.2 Cell viability—mMSCs were seeded onto CS, SCS, CCS and BCS disks (N=6) and cultured for one week. Cell viability was determined with 3-(4,5-dimethylthiazol-2-yl)-2,5-diphenyl tetrazolium bromide (MTT) assay (Cell Proliferation Kit I, Roche, Mannheim, Germany). The formazan content of each well was computed as a percentage of the mean of non-mineralized collagen scaffolds (CS), which was taken to represent 100% cell viability. Experiments were conducted in sextuplicates (N=6).

2.5 *In vitro* osteogenesis

1×10^4 mMSCs were seeded onto each scaffold and cultured in 1.5 mL of culture medium for 24 hr. The medium was changed to osteogenic differentiation medium (culture medium supplemented with 50 μg/mL ascorbic acid, 10 mmol/L β-glycerophosphate, and 100 nmol/L dexamethasone, Sigma-Aldrich). The effects of different scaffolds on osteogenic differentiation of mMSCs were examined with alkaline phosphatase (ALP) assay, alizarin red-S assay and mRNA expressions of marker genes associated with osteogenesis.

2.5.1 ALP assay—mMSC-seeded CS (control), SCS, CCS or BCS scaffolds were cultured in osteogenic differentiation medium for 7 or 14 days (N=6). Alkaline phosphatase activity was determined using a QuantiChrom ALP assay kit (BioAssay Systems, Hayward, CA, USA).

2.5.2 Alizarin red-S assay—Indirect evaluation of the scaffold eluents was performed to prevent interference of the calcium ions in the CCS and BCS scaffolds on alizarin red-S staining. The CS (control), SCS, CCS, or BCS were placed in transwell inserts with 3 μm pore size (BD Falcon, Franklin Lakes, NJ, USA) and exposed to differentiated mMSCs in the lower chamber for 21 days with the osteogenic differentiation medium replenished every 3 days. The cells were then stained with alizarin red-S (40 mM solution; pH 4.2) and then dissolved in 10% acetic acid for quantification (N = 6). Absorbance of the extracts was spectrophotometrically determined at λ= 405 nm. The amount of calcium extracted (in millimoles) was determined using a calibration curve correlating absorbance of alizarin red-S with known calcium concentrations.

2.5.3 mRNA expressions of marker genes associated with osteogenesis—mMSC-seeded CS (control), SCS, CCS or BCS were incubated in osteogenic differentiation medium for 7 days (N=6). Real-time reverse transcription-polymerase chain reaction (qRT-PCR) was used for examining the expression of differentiation makers, [alkaline phosphatase (ALP), collagen I (COLI), osteopontin (OPN) and osteocalcin (OC)], OPG and RANKL. Glyceraldehyde 3-phosphate dehydrogenase (GAPDH) was used as the house-keeping gene. RNA extraction and cDNA synthesis were performed using the RNeasy Mini Kit (QIAGEN, Valencia, CA, USA) and High Capacity cDNA Reverse Transcription Kit (Applied Biosystems, Foster City, CA, USA). qRT-PCR was performed using FastStart Universal SYBR Green Master Kit (Roche Applied Science, Indianapolis, IN, USA) and

forward and reverse primers for the aforementioned genes (Supporting Information, S-Table I), in a 7300 RT-PCR system (Applied Biosystems). Target gene expressions were analyzed using the comparative cycle threshold (ΔΔCt) method after normalization with GAPDH. Fold differences were calculated by comparing with normalized Ct values of the CS control.

2.5.4 Western blot—mMSCs were cultured on CS (control), SCS, CCS or BCS (N=6) for 7 days. The total protein from each group (40 μg) was fractionated by sodium dodecyl sulfate polyacrylamide gel electrophoresis (SDS-PAGE) and transferred onto a nitrocellulose membrane. The latter was blocked with 5% non-fat milk and incubated with primary antibodies against OPG (1:300, 11383, Santa Cruz Biotechnology Inc., Dallas, TX, USA), RANKL (1:300, 7628, Santa Cruz Biotechnology Inc.), β-actin (1:1000, 3700, Cell Signaling Technology, Danvers, MA,USA), Phospho-p44/42 MAPK (p-ERK1/2) (Thr202/Tyr204) (1:800, 4370, Cell Signaling Technology), total-ERK1/2 (1:1000, 4695, Cell Signaling Technology), Phospho-p38 MAPK (Thr180/Tyr182) (1:800, 4511, Cell Signaling Technology), total-p38 (1:1000, 9212, Cell Signaling Technology), Phospho-Akt (Thr308) (1:800, 4056, Cell Signaling Technology) and total-Akt (1:1000, 4691, Cell Signaling Technology). Signals were revealed after incubation with horseradish peroxidase-conjugated secondary antibody (1:5000, Santa Cruz Biotechnology Inc.) and enhanced chemiluminescence detection (GE Healthcare, Piscataway, NJ, USA). The stained bands were scanned and quantified using a densitometer (Syngene Bioimaging System; Frederick, MD, USA) and Scion Image software (Frederick). Protein expression levels were normalized against β-actin for each sample.

2.6 Pathway inhibition

To investigate the signal transduction pathways associated with osteogenesis and inhibition of RANKL-mediated osteoclastogenesis of scaffold-conditioned mMSCs, the mMSCs were pre-treated for 1 hr with 10 μM U0126 (9903, a selective ERK1/2 inhibitor), 10 μM SB203580 (5633, a selective p38 inhibitor), or 50 μM LY294002 (9901, a selective PI3K/Akt inhibitor) in α-MEM medium for blocking of corresponding pathway, and then cultured with BCS in osteogenic differentiation medium with same concentration of aforementioned inhibitors. All inhibitors were obtained from Cell Signaling Technology (Danvers, MA, USA). The inhibitor pre-treatment time and concentration were in accordance with the manufacturer's instruction. The osteogenic differentiation medium with the inhibitors was changed every three days during the experiments. The mMSCs cultured with BCS without inhibitor pre-treatment were used as the control. All inhibitors were obtained from Cell Signaling Technology. The effects of pathway inhibition on osteogenic differentiation of BCS-conditioned mMSCs were examined with alkaline phosphatase assay and alizarin red-S assay after 7 days and 21 days, respectively. The influence of pathway inhibition on the osteoclastogenesis inhibitory effect of BCS-conditioned mMSCs was investigated using Western blot analyses of OPG and RANKL, tartrate-resistant acid phosphatase (TRAP) staining and resorption pit assay, as described in the sections below.

2.7 Effects of scaffold-conditioned mMSCs on osteoclastogenesis and osteoclast function

2.7.1 Preparation of scaffold-conditioned mMSCs—The mMSCs were co-cultured with CS (control), SCS, CCS or BCS in a transwell system (96-well, 0.4μm, Corning), with scaffolds in the lower chamber and mMSCs in the upper chamber for 7 days.

2.7.2 Tartarate-resistant acid phosphatase (TRAP) staining—1×10^4/well RAW 264.7 cells were incubated in α-MEM medium supplemented with 10% fetal bovine serum in 96-well plates for 24 hr. The cells were then co-cultured with the scaffold-conditioned mMSCs in a transwell system (Raw 264.7 cells in the lower chamber and mMSCs in the upper chamber) for 7 days in the presence of 50 ng/mL RANKL (R&D Systems, Abdingdon, UK). For evaluation of osteoclastogenesis, the cells in the lower chamber were fixed with 4% formaldehyde and stained with TRAP (387-A, Sigma-Aldrich). The total number of TRAP-positive multinucleated cells (three or more nuclei for each cell) from ten randomly-selected 400× fields was counted under the light microscope (N=6).

2.7.3 Resorption pit assay—For evaluation of osteoclast functional activity, RAW 264.7 cells (2×10^3/well) were cultured on the top of 1-mm thick, sterilized dentin slices with culture medium at 37 °C for 24 hr, and then co-cultured with scaffold-conditioned mMSCs in the transwell system, together with 50 ng/mL RANKL (R&D Systems) in the culture medium. After 14 days, cells were removed from the dentin slices with sonication for 5 min. The dentin slices were stained with 1% toluidine blue (Sigma-Aldrich) for 2 min, washed with distilled water and observed under a light microscope [24]. Stained resorption pits were visualized as blue areas. The mean area of resorption from six randomly-selected 400× fields was analyzed using Image J (National Institute of Health, Bethesda, MD, USA).

2.7.4 Effects of OPG neutralization—To examine the effects of OPG neutralization on osteoclastogenesis inhibition and osteoclast activity reduction of BCS-conditioned mMSCs, the TRAP-staining and resorption pit experiments were repeated by adding 1μg/mL of OPG-neutralizing antibody (MAB805, R&D systems) to the RANKL-containing culture medium prior to co-culturing.

2.7.5 Effects of pathway inhibition—To examine the effects of pathway inhibition on RANKL-mediated osteoclastogenesis and osteoclast function, mMSCs were first pretreated with 10 μM U0126 (selective ERK1/2 inhibitor), 10 μM SB203580 (selective p38 inhibitor), or 50 μM LY294002 (selective Akt inhibitor) in α-MEM medium for 1 hr and then co-cultured with BCS in the transwell system as mentioned in 2.7.1. The culturing medium with the same concentration of aforementioned inhibitors was changed at the 3rd day during the experiments. Seven days later, the transwell inserts with the conditioned mMSCs were exposed to pre-established RAW 264.7 cells. The TRAP-staining and resorption pit experiments were repeated as described above.

2.8 Statistical analyses

Data for each assay were analyzed with one-way analysis of variance (ANOVA) and Holm-Sidak multiple comparison tests to examine the effects of various scaffolds on the parameter investigated. If the normality and homoscedasticity assumptions of the data set were

violated, the corresponding data were non-linearly transformed to satisfy those assumptions prior to the use of parametric statistical methods. When non-linear transformation was unsuccessful in satisfying those assumptions, the data set involved was analyzed using Kruksal-Wallis ANOVA and Dunn's multiple comparison tests. For all tests, statistical significance was preset at $\alpha = 0.05$.

3. Results

3.1 Intrafibrillar mineralization

Collagen scaffolds mineralized intrafibrillarly with single mineral phases are shown in the top panels of Figure 1A (SCS using poly(allylamine) hydrochloride-stabilized silicic acid as building blocks; CCS using poly(aspartic acid) stabilized-amorphous calcium phosphate as building blocks). Collagen scaffolds that were first silicified prior to calcification (BCS) demonstrated intrafibrillar silica-apatite biphasic minerals within the collagen matrix. During the initial stage of biphasic mineralization (4 days), both intrafibrillar apatite platelets and the banding characteristics of silicified collagen could be discerned (Figure 1A, BCS-early stage). At 7 days, most of the intrafibrillar spaces were occupied by elongated electron-dense crystallites, masking the cross-banding structure of the silicified collagen fibrils (Figure 1A, BCS-late stage). Selected area electron diffraction indicates the crystalline feature of the newly formed minerals, with diffraction patterns that are characteristic of apatite. Presence of Si, O, Ca and P elements inside the bisphasic mineralized collagen fibrils had previously been confirmed using TEM-based elemental analysis [23].

3.2 Release of silicic acid and calcium ions

Cumulative release profiles of silicic acid from SCS and BCS, and calcium ions from CCS and BCS are shown in Figure 1B. The SCS and BCS showed a similar silicic acid releasing profile, with a burst release phase in the first day (about 12 ppm) and reaching a plateau over the subsequent 6 days. Release of calcium ions from BCS was characterized by a more gradual increase in cumulative calcium ion concentration with increased exposure time. The calcium release from CCS was similar to that of BCS.

3.3 Cell proliferation/viability

The DNA contents and succinic dehydrogenase activities of mMSCs seeded on the scaffolds and cultured for one week did not show any significant differences among the different mineralized scaffolds ($P > 0.05$; Figure 1C).

3.4 *In vitro* osteogenesis

3.4.1 ALP assay and alizarin red-S assay—Alkaline phosphatase activity of mMSCs exposed to different scaffolds at 7 days and 14 days (Figure 2A) was significantly different among groups for both time points ($P < 0.001$). For each time period, the BCS group exhibited the highest ALP activity while the CS control exhibited the lowest activity. No significant difference was observed between the SCS group and CCS group for both time points.

Representative alizarin red-S staining of extracellular calcified deposits produced by mMSCs after they were cultivated with CS, SCS, CCS or BCS in osteogenic differentiation medium for 21 days is shown in Figure 2B. The BCS group showed the highest calcium ion concentration derived from the deposits ($P < 0.05$). The extent of extracellular calcified deposits formation in the CCS group was not significantly different from the CS negative control, but was significantly lower than the SCS group ($P < 0.05$).

3.4.2 mRNA expressions of osteogenesis-associated marker genes—The mRNA expressions of osteogenic differentiation markers, (alkaline phosphatase, collagen I, osteopontin and osteocalcin), OPG and RANKL, as determined with qRT-PCR, are show in Figure 2C. Expression of alkaline phosphatase in the CCS group was significantly lower than that of the SCS group, which, in turn, was significantly lower than the BCS group ($P < 0.05$). The expression levels of osteopontin and OPG of the differentiated mMSCs was in the order CCS < SCS < BCS ($P < 0.05$). Expressions of osteocalcin in the CCS and BCS groups were not significantly different, but were significantly higher than the SCS group ($P < 0.05$). The expression level of RANKL was significantly down-regulated in the SCS and BCS groups ($P < 0.05$), with no significant difference between the two groups.

3.5 Osteogenesis-related signaling pathways

The effects of scaffolds on osteogenesis-related signal transduction pathways, as indicated by the expression of p-ERK, p-p38 and p-Akt, are shown in Figures 3A and 3B. Significant differences in p-ERK expression were detected among the 4 groups ($P < 0.05$), with BCS group being the highest and CS negative control being the lowest. For the expression of p-p38, the BCS group was significantly higher than the other groups ($P < 0.05$). There was no significant difference between the CS and CCS groups, both of which were significantly lower than the SCS group ($P < 0.05$). Expressions of p-Akt in the CCS and BCS groups were significantly higher than the CS and SCS groups ($P < 0.05$).

After the use of pathway inhibitors (U0126 against ERK, SB203580 against p38 or LY294002 against Akt) on BCS-conditioned mMSCs, the alkaline phosphatase activity of the stem cells was assessed after 7 days (Figure 3C), while the Ca concentration of extracellular calcified deposits was assessed with the alizarin red-s assay after 21 days (Figure 3D). Whereas significant reductions in alkaline phosphatase activity and Ca concentration were observed for U0126 and SB203580 ($P < 0.05$), there was no significant reduction in both alkaline phosphatase activity and Ca concentration level in mMSCs exposed to BCS, or in mMSCs that were inhibited with LY294002 prior to their exposure to BCS. That is, the LY294002 inhibitor against the Akt signaling pathway had no inhibition effect on osteogenesis.

3.6 Effects of scaffold-conditioned mMSCs on osteoclastogenesis and osteoclast function

Up-regulation of OPG expression, increase in the OPG/RANKL ratio, and down-regulation of RANKL expression were significantly more pronounced in the BCS and SCS groups (Figures 4A; $P < 0.05$). These effects were significantly more prominent for BCS compared with SCS. The number of TRAP-positive osteoclasts and the resorption pits on the surface of dentin slices were significantly lower in the SCS and BCS groups ($P < 0.05$) when

compared with the CS and CCS groups (Figure 4, B and C). The inhibitory effects of the BCS-conditioned mMSCs on osteoclastogenesis and osteoclast function were no longer significant after the stem cells were treated with OPG-neutralizing antibody ($P > 0.05$).

3.7 Effects of pathway inactivation on RANKL-mediated osteoclastogenesis and osteoclast function

To identify the effects of signaling pathway inactivation on OPG and RANKL protein expression, and on differentiation inhibition of osteoclast precursors by BCS-conditioned mMSCs, the stem cells were treated with U0126 against ERK, SB203580 against p38 or LY294002 against Akt. The U0126 inhibitor against the ERK pathway had no significant effect on OPG and RANKL expressions (Figure 5A), as well as on the number of TRAP positive cells and the area of resorption pits (Figure 5, B–D). In contrast, inhibition of the p38 pathway by SB203580 resulted in significant decrease in OPG expression and OPG/RANKL ratio (Figure 5A), as well as significant increases in TRAP-positive cells and resorption pit formation. Although inhibition of the Akt pathway by LY294002 produced similar rescuing effects, the results were less significant than those resulting from inhibition of the p38 pathway by SB203580 (Figure 5, B–D; $P < 0.05$ for all analyses).

4. Discussion

There is a tendency in contemporary tissue engineering to mimic biological processes for producing bone replacement scaffolds. With improvements in the understanding of how biomineralization occurs in nature, it is possible to create mineralized collagen scaffold containing intrafibrillar apatite only, intrafibrillar silica only, or biphasic intrafibrillar mineral phases. Examining the biological effects of these mineralized collagen scaffolds provides insight on the contributions of intrafibrillar silica and intrafibrillar apatite, and the potential synergistic effects of these two intrafibrillar minerals on the anabolic and catabolic aspects of bone metabolism.

Silicon is an essential trace element for metabolic processes associated with connective tissue development and bone metabolism [25–27]. Ample reports are available that examined the effects of Ca- and Si-containing biomaterials in promoting or suppressing the differentiation of osteoblast or osteoclast precursors. These materials include Si-substituted apatite [28,29], bioactive glasses [12,30] and calcium silicate cements [31,32]. While all of these materials were found to stimulate differentiation of osteoblast precursors and bone formation, their effects on osteoclastogenesis and cell-mediated bone degradation were ambiguous and appeared to be material-dependent. As a tissue engineering scaffold for repairing minimal stress-bearing defects, the dynamic mechanical properties of BCS are superior to CCS because of its reduced brittleness and increased resilience [23]. However, the biological effects of the BCS have yet to be elucidated. Bone marrow-derived MSCs represents an optimal cellular source for seeding of bone tissue engineering scaffolds due to their potential for osteogenic differentiation and in modulating RANKL-mediated osteoclastogenesis. It is important to understand from an *in vitro* perspective how interactions with intrafibrillar mineral-containing collagen scaffolds may affect the osteogenic differentiation potential of MSCs, as well as the ability of MSCs to modulate

RANKL-mediated osteoclast differentiation from mononuclear precursor cells and the activity of the differentiated osteoclast-like cells.

Osteogenic differentiation of CCS-conditioned mMSCs resulted only in moderate increases in ALP activity but no significant increase in calcium deposition when compared to the CS control (Figure 2, A and B). By contrast, both activities were significantly increased when mMSCs were exposed to SCS and BCS, particularly for BCS. Thus, the first null hypothesis that there is no difference among the unmineralized and mineralized collagen scaffolds with different intrafibrillar minerals in stimulating osteogenesis of mMSCs has to be rejected. The hypothesis was further tested by evaluating the osteogenesis associated gene markers, including ALP, COLI, OPN and OC. It is known that ALP acts as an early indicator of cellular activity and differentiation, and generates inorganic phosphate which is needed for hydroxyapatite crystallization in the bone matrix. Collagen I is an important component of bone extra-cellular matrix, on which the differentiating cells can find their functional destination within a growing bone structure. OPN and OC are important noncollagenous proteins which play important roles in the differentiation of osteoblast progenitor cells, with significant up-regulation observed in both matrix synthesis and mineralization [33]. A similar trend was also observed at the mRNA level, as reflected by up-regulation of the expression of osteoblast lineage-specific phenotypic markers ALP, COL I and OPN by SCS and BCS (Figure 2C). Taken together, these results indicate that collagen scaffolds containing amorphous silica are more osteoinductive compared to unmineralized or calcified collagen scaffolds. Moreover, ALP activity, *in vitro* bone nodule formation and osteogenesis related gene expression in the BCS group were all significantly higher than those in the SCS group. This may be caused by the synergy of both Ca and Si from the BCS. The physicochemical features of the scaffolds, such as surface chemistry, roughness, stiffness and nanomaterial alignment may also contribute to the differences in osteogenic differentiation of mMSCs in different groups. Further studies are needed to investigate the effect of substrate surface characteristics and scaffold bulk properties on both short-term stem cell adhesion, spreading and proliferation, and longer-term lineage differentiation, functionalization and viability.

Multiple signaling pathways are involved in the osteogenic differentiation of mesenchymal stem cells, including the mitogen-activated protein kinase (MAPK), phosphatidylinositol-3 kinase (PI3K)-Akt, TGF-β/BMP, and Wnt/β-Catenin pathways [34]. Both MAPK and PI3K/Akt pathways have been considered as the upstream of integrin-mediated signaling cascades induced by extracellular stimuli such as calcium [32,35], silicon [32] and strontium [36]. The MAPK cascades are one of the most thoroughly studied signal transduction systems, and have been shown to participate in a diverse array of cellular activities, including cell differentiation, movement, division, and programed cell death [32,36]. It was reported that the MAPK/ ERK and p38 kinases signaling pathways of human MSCs were significantly activated when the cells were exposed to a calcium silicate cement with high silica content [32]. The PI3K pathway controls the metabolism of inositol phospholipids and regulates many fundamental cellular processes, including cell growth, proliferation, and survival. Protein kinase B (Akt) is an intermediate downstream lipid product generated by PI3K, which, upon activation by phosphorylation, regulates other downstream pathways to

facilitate cell function [37]. To understand the potential signaling pathways involved during osteogenic differentiation of mMSCs in the presence of different collagen scaffolds, the degree of phosphorylation of ERK and p38 kinases and Akt kinases were examined after the mMSCs were induced to differentiate in the presence of the four scaffolds. When mMSCs were cultured in osteogenic differentiation medium in the presence of the collagen scaffolds, both the ERK and p38 phosphorylation levels were increased, in the order BCS > SCS > CCS (Figure 3, A and B), while the phosphorylation levels of Akt were less clear-cut. Based on these results, it is surmised that osteogenic differentiation in the presence of mineralized collagen scaffolds proceeds via the activation of the ERK and p38 pathways; this speculation was further validated using pathway inhibitors (Figure 3, C and D). Osteogenic differentiation was more pronounced in the BCS group compared with the SCS group because both Ca ions and silicic acid released from those scaffolds were capable of activating the ERK pathway. By contrast, the p38 pathway was activated only by silicic acid but not Ca ions. When pathways were blocked by their respective inhibitors during culturing of mMSCs with BCS, blocking the ERK pathway decreased mMSC differentiation capacity (ALP and Ca deposition) to levels that were not significantly different from the CS control (Figure 3, C and D). Both ALP expression and Ca deposition were significantly higher than the CS control group when the p38 pathway was blocked. These results further validated that the ERK pathway is predominantly involved, while the p38 pathway is subsidiary in promoting osteogenic differentiation of mMSCs by BCS. Conversely, there was no decrease in ALP activity or Ca deposition upon inhibition of the Akt pathway, indicating that this pathway was not activated during osteogenic differentiation.

Several recent studies suggested that soluble products derived from biosilica inhibit the differentiation of osteoclasts from their precursors via altering the differential expression of OPG and RANKL by osteoblast-lineage cells [12,17–19]. In the present work, amorphous silica-containing SCS and BCS up-regulated OPG expression and down-regulated RANKL expression in mMSCs at both the gene (Figure 2C) and protein level (Figure 4A). In contrast, these effects were not exhibited by CCS or the CS control. As a consequence of the net increase in OPG/RANKL ratios in the SCS and BCS groups, RANKL-mediated osteoclastogenesis (TRAP staining) and functioning of the differentiated osteoclast-like cells (resorption pit assay) were inhibited after the RAW 264.7 precursors were co-cultured with SCS-conditioned or BCS-conditioned mMSCs (Figure 4, B and C). The inhibitory effects of SCS-conditioned or BCS-conditioned mMSCs on RANKL-mediated osteoclastogenesis and osteoclast function were further established when the increase in OPG expression by BCS-conditioned mMSCs was antagonized by anti-OPG antibodies (Figure 4, B and C). These results warrant rejection of the second null hypothesis that there is no difference among the various collagen scaffolds in their indirect inhibition of RANKL-mediated osteoclastogenesis and osteoclast function.

When BCS-conditioned mMSCs were treated with the respective inhibitors of the ERK/MAPK, p38/MAPK and PI3K/Akt pathways (Figure 5A), up-regulation of OPG expression and increase in OPG/RANKL ratio in mMSCs were more significantly inhibited by blocking the p38 pathway, and less significantly inhibited by blocking the Akt pathway. These pathway-related effects were also reflected by the results of TRAP staining and resorption pit analysis (Figure 5, B and C). Taken together, the results indicate that the p38 pathway is

predominantly involved, while the Akt pathway is subsidiary in inhibiting RANKL-mediated osteoclastogenesis and osteoclast function by BCS-conditioned mMSCs. While these results are supportive of the involvement of the p38/MAPK pathway in RANKL-mediated osteoclastogenesis [38], communication between the Akt and p38 pathways may result in their reciprocal augmentation when both pathways are activated [39]. Whereas BCS induced the activation of both the p38 and Akt pathways in mMSCs, CCS activated only the Akt pathway but had no effect on the p38 pathway (Figure 3B). Without the incorporation of intrafibrillar silica, CCS alone could not up-regulate OPG expression by mMSCs (Figure 4A), and had no significant inhibitory effect on MSC-induced osteoclastogenesis or osteoclast function (Figure 4, B and C). This is probably due to the inability of CCS to activate the p38 signaling pathway. On the contrary, when biphasic minerals were incorporated into collagen scaffolds, the effect of Ca ion release on activation of the Akt pathway became apparent because the p38 pathway was concurrently activated by the release of silicic acid from BCS, enabling cross-talks between the Akt and p38 pathways. This probably explains why the effects of OPG expression, RANKL-mediated osteoclastogenesis and osteoclast function were more significantly manifested by BCS-conditioned mMSCs, compared with SCS-conditioned mMSCs (Figure 4). Other signal transduction pathways not investigated in the present study may also be involved, such as inhibition of RANKL-mediated osteoclastogenesis by canonical Wnt/β-catenin signaling of osteoblastic-lineage cells [40]. In addition, the osteoclastogenesis experiments in the present study were conducted using RAW 264.7 cells, which may give different results than primary osteoclasts from bone marrow macrophages. Further studies need to be performed to clarify the effect of the scaffolds on the cross-talk between primary osteoblasts and osteoclasts from bone marrow.

From a tissue engineering perspective, a scaffold that possesses the ability to inhibit RANKL-mediated osteoclastogenesis after implantation into a bone defect is highly desirable because of the requisition for anabolic over catabolic processes during this initial phase of bone metabolism. However, a balance between these two processes must be accomplished subsequently for maintenance of long-term bone health. Thus future studies will focus on the long-term regulation of biphasic mineralized collagen scaffolds on both osteogenesis and osteoclastogenesis.

5. Conclusion

For the biomimetic mineralized collagen scaffolds, the intrafibrillar silica and intrafibrillar apatite have different effects on the anabolic and catabolic aspects of bone metabolism. Apart from its mechanical function in incorporating resilience into a mineralized collagen matrix, intrafibrillar silica appears to play a more bioactive, dual functional role in bone metabolism. This dual functional role of intrafibrillar silica is manifested by the release of silicic acid, which exerts stimulatory effects on the osteogenic differentiation of MSCs, and inhibitory effects on the ability of MSCs to modulate RANKL-mediated osteoclastogenesis via increase in their OPG expression. Apart from its mechanical function in providing stiffness to a mineralised collagen matrix, intrafibrillar apatite in a biphasic mineralised collagen scaffold appears to interact synergistically with intrafibrillar silica in enhancing MSC differentiation by activating ERK/MAPK pathway. In addition, the intrafibrillar

apatite also play a supportive role in inhibiting RANKL-mediated osteoclastogenesis, by activating the PI3K/Akt signalling pathway in MSCs to further up-regulate OPG expression induced by intrafibrillar silica via activation of the p38/MAPK pathway. Collectively, incorporation of biphasic intrafibrillar silica and apatite mineral phases enhances both the mechanical and biological properties of collagen scaffolds for repair of bony defects.

Supplementary Material

Refer to Web version on PubMed Central for supplementary material.

Acknowledgments

This work was supported by grant R01 DE015306-06 from NIDCR (PI. David H Pashley), grant 81130078 (PI. Jihua Chen), 81400555 (PI. Lina Niu) and 81300898 (PI. Kai Jiao) from National Nature Science Foundation of China and program No. IRT13051 for Changjiang Scholars and Innovative Research Team in University. The murine mesenchymal stem cells employed in this work were provided by the Texas A&M Health Science Center College of Medicine Institute for Regenerative Medicine at Scott & White through a grant from NCRR of the NIH, Grant #P40RR017447.

References

1. Liu Y, et al. Hierarchical intrafibrillar nanocarbonated apatite assembly improves the nanomechanics and cytocompatibility of mineralized collagen. Adv Func Mater. 2013; 23:1404–1411.
2. Gupta HS, Seto J, Wagermaier W, Zaslansky P, Boesecke P, Fratzl P. Cooperative deformation of mineral and collagen in bone at the nanoscale. Proc Natl Acad Sci U S A. 2006; 103:17741–17746. [PubMed: 17095608]
3. Alexander B, Daulton TL, Genin GM, Lipner J, Pasteris JD, Wopenka B, Thomopoulos S. The nanometre-scale physiology of bone: steric modelling and scanning transmission electron microscopy of collagen-mineral structure. J R Soc Interface. 2012; 9:1774–1786. [PubMed: 22345156]
4. Nudelman F, Bomans PH, George A, de With G, Sommerdijk NA. The role of collagen in bone apatite formation in the presence of hydroxyapatite nucleation inhibitors. Nat Mater. 2010; 9:1004–1009. [PubMed: 20972429]
5. Olszta MJ, et al. Bone structure and formation: a new perspective. Mater Sci Eng. 2007; R58:77–116.
6. Deshpande AS, Beniash E. Bio-inspired synthesis of mineralized collagen fibrils. Cryst Growth Des. 2008; 8:3084–3090.
7. Liu Y, et al. Intrafibrillar collagen mineralization produced by biomimetic hierarchical nanoapatite assembly. Adv Mater. 2011; 23:975–980. [PubMed: 21341310]
8. Zhou GS, Su ZY, Cai YR, Liu YK, Dai LC, Tang RK, Zhang M. Different effects of nanophase and conventional hydroxyapatite thin films on attachment, proliferation and osteogenic differentiation of bone marrow derived mesenchymal stem cells. Biomed Mater Eng. 2007; 17:387–395. [PubMed: 18032820]
9. Liu Y, Wang G, Cai Y, Ji H, Zhou G, Zhao X, Zhang M. In vitro effects of nanophase hydroxyapatite particles on proliferation and osteogenic differentiation of bone marrow-derived mesenchymal stem cells. J Biomed Mater Res A. 2009; 90:1083–1091. [PubMed: 18671263]
10. Niu LN, et al. Infiltration of silica inside fibrillar collagen. Angew Chem Int Ed Engl. 2011; 50:11688–11691. [PubMed: 21983995]
11. Niu LN, et al. Biomimetic silicification of demineralized hierarchical collagenous tissues. Biomacromolecules. 2013; 14:1661–1668. [PubMed: 23586938]

12. Mladenovic Ž, Johansson A, Willman B, Shahabi K, Björn E, Ransjö M. Soluble silica inhibits osteoclast formation and bone resorption in vitro. Acta Biomater. 2014; 10:406–418. [PubMed: 24016843]
13. Reffitt DM, et al. Orthosilicic acid stimulates collagen type 1 synthesis and osteoblastic differentiation in human osteoblast-like cells in vitro. Bone. 2003; 32:127–135. [PubMed: 12633784]
14. Wiens M, et al. Osteogenic potential of biosilica on human osteoblast-like (SaOS-2) cells. Calcif Tissue Int. 2010; 87:513–524. [PubMed: 20725824]
15. Wang Y, Wang WL, Xie WL, Li LZ, Sun J, Sun WJ, Gong HY. Puerarin stimulates proliferation and differentiation and protects against cell death in human osteoblastic MG-63 cells via ER-dependent MEK/ERK and PI3K/Akt activation. Phytomedicine. 2013; 20:787–796. [PubMed: 23639192]
16. Rodríguez-Carballo E, et al. The p38α MAPK function in osteoprecursors is required for bone formation and bone homeostasis in adult mice. PLoS One. 2014; 9:e102032. [PubMed: 25007355]
17. Beck GR Jr, Ha SW, Camalier CE, Yamaguchi M, Li Y, Lee JK, Weitzmann MN. Bioactive silica-based nanoparticles stimulate bone-forming osteoblasts, suppress bone-resorbing osteoclasts, and enhance bone mineral density in vivo. Nanomedicine. 2012; 8:793–803. [PubMed: 22100753]
18. Schröder HC, Wang XH, Wiens M, Diehl-Seifert B, Kropf K, Schloßmacher U, Müller WE. Silicate modulates the cross-talk between osteoblasts (SaOS-2) and osteoclasts (RAW 264.7 cells): inhibition of osteoclast growth and differentiation. J Cell Biochem. 2012; 113:3197–3206. [PubMed: 22615001]
19. Wiens M, Wang X, Schröder HC, Kolb U, Schlossmacher U, Ushijima H, Müller WE. The role of biosilica in the osteoprotegerin/RANKL ratio in human osteoblast-like cells. Biomaterials. 2010; 31:7716–7725. [PubMed: 20673584]
20. Lee SE, Woo KM, Kim SY, Kim HM, Kwack K, Lee ZH, Kim HH. The phosphatidylinositol 3-kinase, p38, and extracellular signal-regulated kinase pathways are involved in osteoclast differentiation. Bone. 2002; 30:71–77. [PubMed: 11792567]
21. Takami M, Cho ES, Lee SY, Kamijo R, Yim M. Phosphodiesterase inhibitors stimulate osteoclast formation via TRANCE/RANKL expression in osteoblasts: possible involvement of ERK and p38 MAPK pathways. FEBS Lett. 2005; 579:832–838. [PubMed: 15670856]
22. Niu LN, et al. Intrafibillarly-silicified collagen scaffolds for SDF-1 mediated stem cell homing in hard tissue regeneration. FASEB J. 2012; 26:4517–4529. [PubMed: 22859369]
23. Niu LN, et al. Multiphase intrafibrillar mineralization of collagen. Angew Chem Int Ed Engl. 2013; 52:5762–5766. [PubMed: 23606345]
24. Cho ES, Kim MK, Son YO, Lee KS, Park SM, Lee JC. The effects of rosiglitazone on osteoblastic differentiation, osteoclast formation and bone resorption. Mol Cells. 2012; 33:173–181. [PubMed: 22286232]
25. Carlisle EM. Silicona possible factor in bone calcification. Science. 1970; 167:279–280. [PubMed: 5410261]
26. Macdonald HM, Hardcastle AC, Jugdaohsingh R, Fraser WD, Reid DM, Powell JJ. Dietary silicon interacts with oestrogen to influence bone health: evidence from the Aberdeen Prospective Osteoporosis Screening Study. Bone. 2012; 50:681–687. [PubMed: 22173054]
27. Kim EJ, Bu SY, Sung MK, Choi MK. Effects of silicon on osteoblast activity and bone mineralization of MC3T3-E1 cells. Biol Trace Elem Res. 2013; 152:105–112. [PubMed: 23306944]
28. Botelho CM, et al. Differentiation of mononuclear precursors into osteoclasts on the surface of Si-substituted hydroxyapatite. J Biomed Mater Res A. 2006; 78:709–720. [PubMed: 16739170]
29. Thian ES, Huang J, Best SM, Barber ZH, Brooks RA, Rushton N, Bonfield W. The response of osteoblasts to nanocrystalline silicon-substituted hydroxyapatite thin films. Biomaterials. 2006; 27:2692–2698. [PubMed: 16423389]
30. Hoppe A, Güldal NS, Boccaccini AR. A review of the biological response to ionic dissolution products from bioactive glasses and glass-ceramics. Biomaterials. 2011; 32:2757–2774. [PubMed: 21292319]

31. Hashiguchi D, et al. Mineral trioxide aggregate inhibits osteoclastic bone resorption. J Dent Res. 2011; 90:912–917. [PubMed: 21531916]
32. Shie MY, Ding SJ. Integrin binding and MAPK signal pathways in primary cell responses to surface chemistry of calcium silicate cements. Biomaterials. 2013; 34:6589–6606. [PubMed: 23768900]
33. Wang X, Schröder HC, Wiens M, Ushijima H, Müller WE. Bio-silica and bio-polyphosphate: applications in biomedicine (bone formation). Curr Opin Biotechnol. 2012; 23:570–578. [PubMed: 22366413]
34. Liu D, et al. Activation of multiple signaling pathways during the differentiation of mesenchymal stem cells cultured in a silicon nanowire microenvironment. Nanomedicine. 2014; 10:1153–1163. [PubMed: 24566272]
35. Magno AL, Ward BK, Ratajczak T. The calcium-sensing receptor: a molecular perspective. Endocr Rev. 2011; 32:3–30. [PubMed: 20729338]
36. Saidak Z, Marie PJ. Strontium signaling: molecular mechanisms and therapeutic implications in osteoporosis. Pharmacol Ther. 2012; 136:216–226. [PubMed: 22820094]
37. Wang C, Lin K, Chang J, Sun J. Osteogenesis and angiogenesis induced by porous β-CaSiO(3)/PDLGA composite scaffold via activation of AMPK/ERK1/2 and PI3K/Akt pathways. Biomaterials. 2013; 34:64–77. [PubMed: 23069715]
38. Matsumoto M, Sudo T, Saito T, Osada H, Tsujimoto M. Involvement of p38 mitogen-activated protein kinase signaling pathway in osteoclastogenesis mediated by receptor activator of NF-kappa B ligand (RANKL). J Biol Chem. 2000; 275:31155–31161. [PubMed: 10859303]
39. Gonzalez I, et al. Akt2, a novel functional link between p38 mitogen-activated protein kinase and phosphatidylinositol 3-kinase pathways in myogenesis. Mol Cell Biol. 2004; 24:3607–3622. [PubMed: 15082758]
40. Spencer GJ, Utting JC, Etheridge SL, Arnett TR, Genever PG. Wnt signalling in osteoblasts regulates expression of the receptor activator of NFkappaB ligand and inhibits osteoclastogenesis in vitro. J Cell Sci. 2006; 119:1283–1296. [PubMed: 16522681]

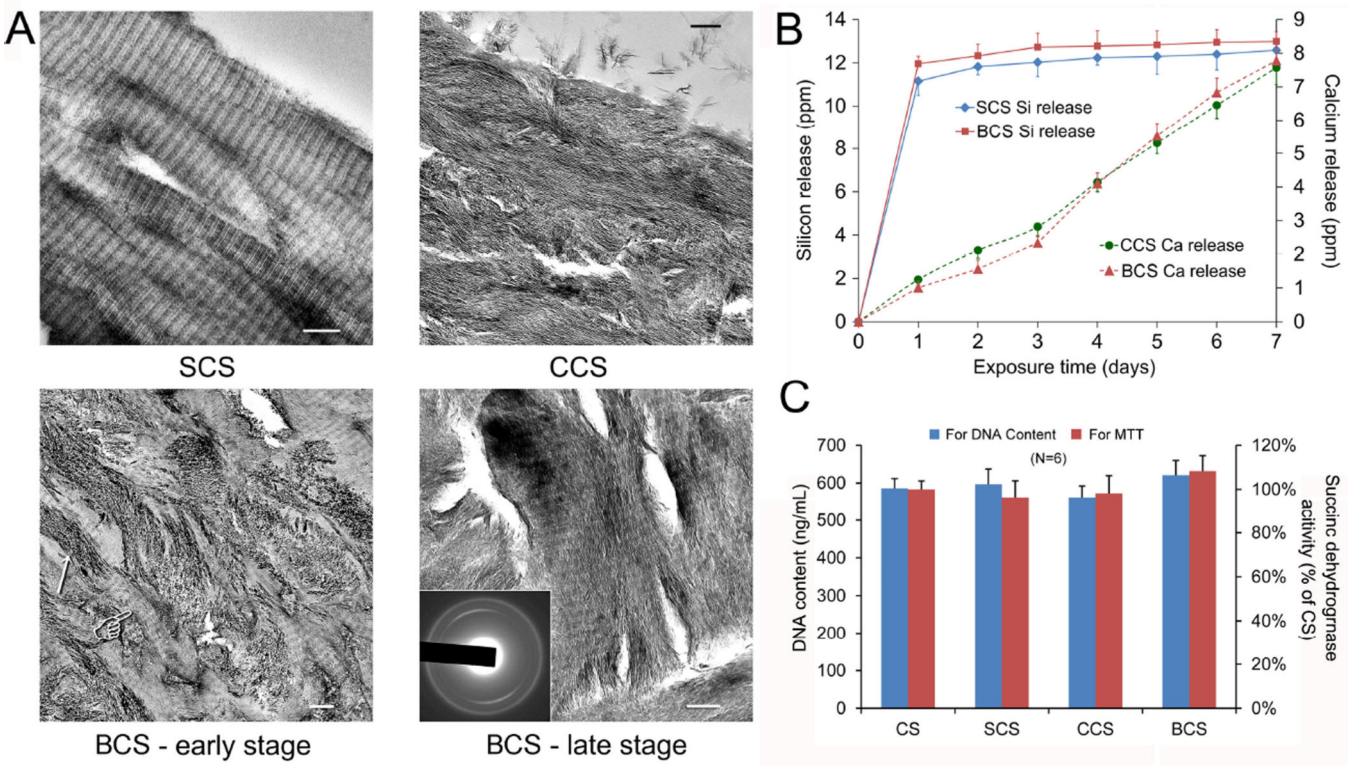

Figure 1.

A. Unstained TEM images of silicified (SCS, upper left panel), calcified (CCS, upper right panel) and biphasic mineralized (lower panels BSC) collagen scaffolds (bar = 200 nm). **BCS-early stage** (4 days): During the initial stage of biphasic mineralization, growth of apatite crystallites (arrow) within the collagen fibrils partially masked the cross banding appearance (pointer) of silicified collagen. **BCS-late stage** (7 days): Most of the remaining intrafibrillar spaces previously not occupied by intrafibrillar silica were filled with apatite crystallites. Inset: selected area electron diffraction showing diffraction patterns that are characteristic of apatite. **B**. Cumulative release profiles of silicic acid from SCS and BCS, and calcium ions from CCS and BCS over one week. **C**. Proliferation and viability of mMSCs after exposure to different collagen scaffolds as determined using DNA content assay and MTT assay. Mitochondrial succinic dehydrogenase activities were normalized against the results obtained from the unmineralised collagen scaffolds (CS; control), which were taken to be 100%.

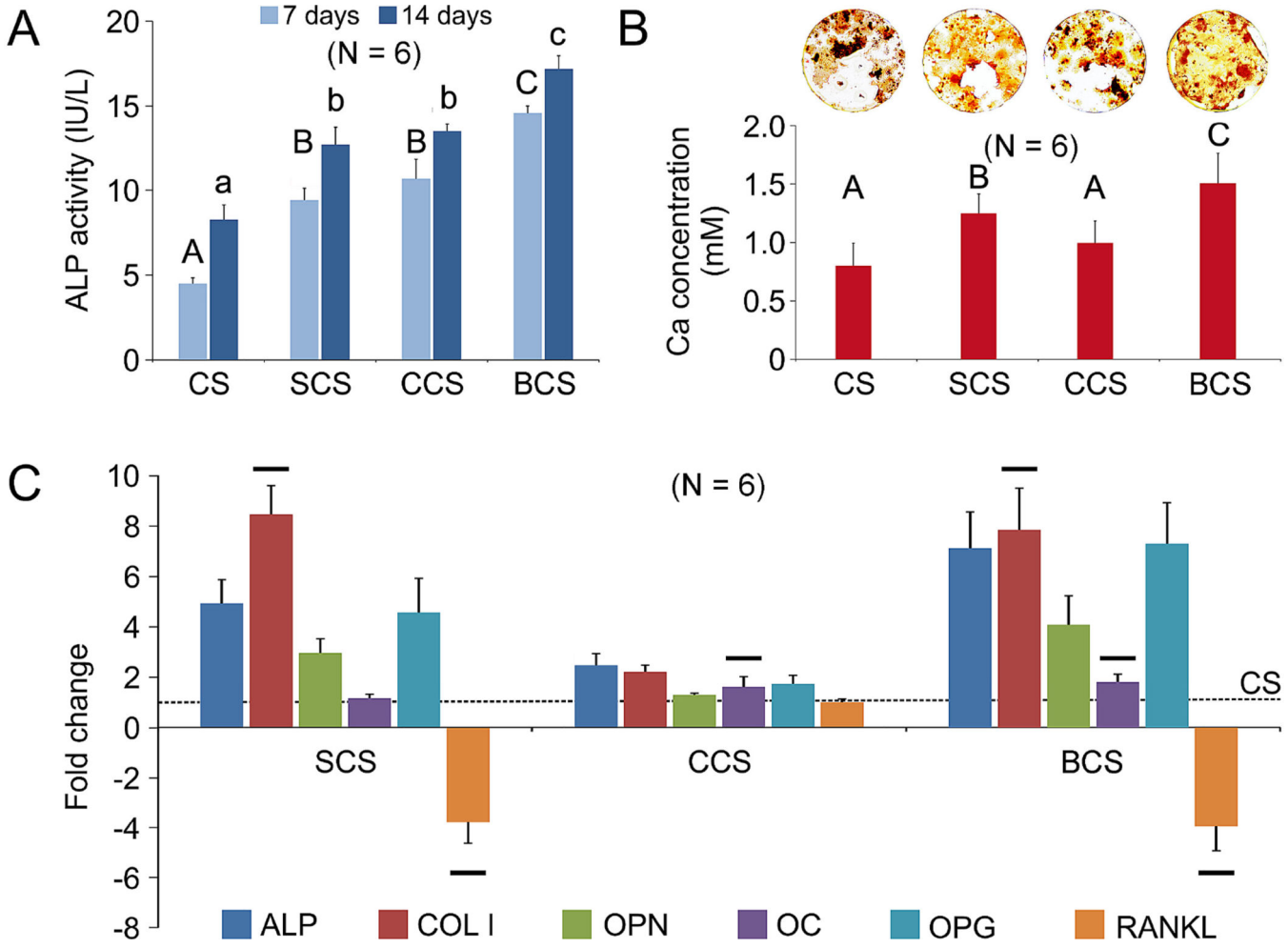

Figure 2.

A. Alkaline phosphatase (ALP) activities of mMSCs cultured with CS, SCS, CCS or BCS in osteogenic differentiation medium for 7 and 14 days. Groups identified with the same upper case letter (for 7 days) or lower case letter (for 14 days) are not significantly different ($P > 0.05$). **B**. Representative alizarin red-S staining (top) of extracellular bone nodules produced by mMSCs after they were cultivated with CS, SCS, CCS or BCS in osteogenic differentiation medium for 21 days. Bar chart (bottom) depicts the extent of osteogenesis in the form of calcium concentrations. Groups identified with the same upper case letter are not significantly different ($P > 0.05$). **C**. qRT-PCR results showing fold regulation of gene markers associated with osteogenic differentiation, bone formation and metabolism, after mMSCs were exposed to CS, SCS, CCS or BCS for 1 week. Gene markers examined were: alkaline phosphatase (*ALP*), Collagen I (*COLI*), osteopontin (*OPN*), osteocalcin (*OCN*), osteoprotegerin (*OPG*), and receptor activator of NF-κB ligand (*RANKL*). Glyceraldehyde 3-phosphate dehydrogenase (*GAPDH*) was used as the endogenous control. Fold regulations (relative to CS negative control) >1 indicate up-regulation while values <−1 indicate down-regulation. For the same gene marker, groups identified with the same horizontal bars are not significantly different ($P > 0.05$).

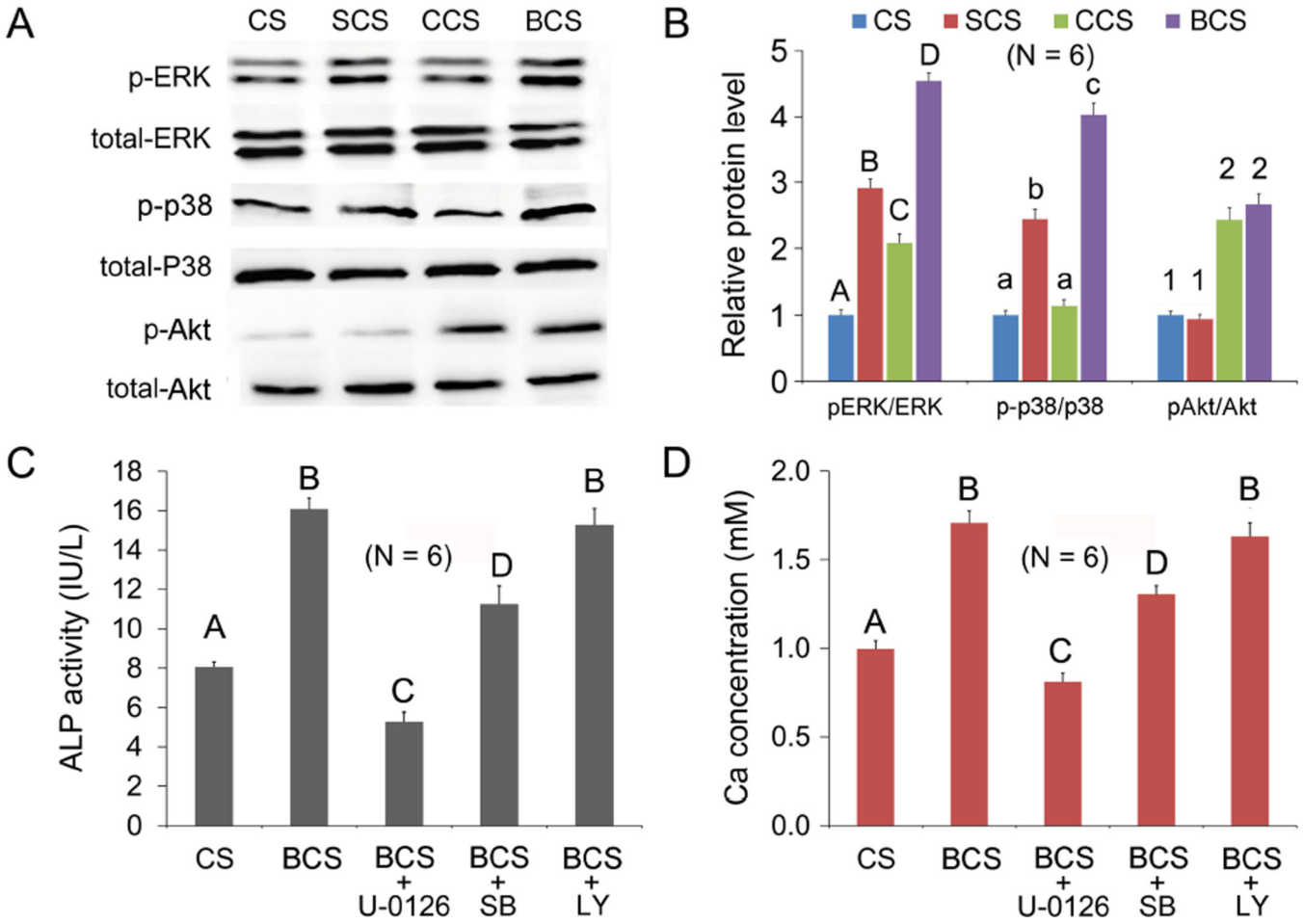

Figure 3.

A Western blot of p-ERK, p-p38 and p-Akt secreted by mMSCs exposed to different scaffolds (CS, SCS, CCS or BCS). **B**. Expressions of p-ERK, p-p38 and p-Akt were normalized against the corresponding protein levels in mMSCs exposed to the CS negative control. For each protein, groups identified with the same upper case letters, lower case letters or numbers are not significantly different ($P > 0.05$). **C and D**. Alkaline phosphatase (ALP; Fig.3C) activities and alizarin red-S staining (Fig.3D) of mMSCs when cultured with biphasic mineralized collagen scaffolds (BCS) before and after the addition of U0126, SB203580 (SB) or LY294002 (LY), the respective inhibitors for ERK, p38 and Akt signaling pathways. mMSCs cultured with collagen scaffolds (CS) served as the negative control. Groups identified with the same upper case letter are not significantly different ($P > 0.05$).

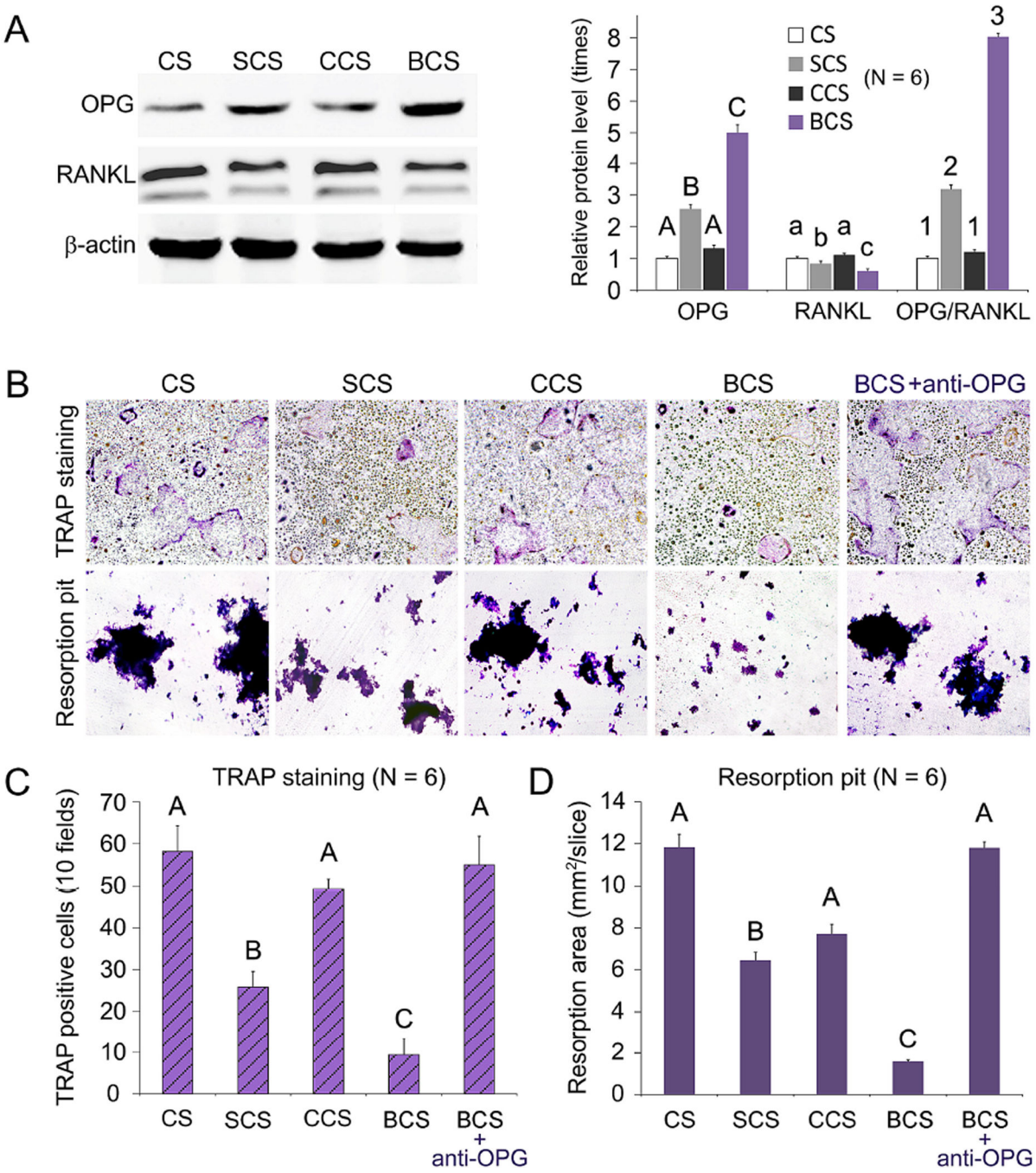

Figure 4.

Effects of scaffold-conditioned osteoblasts on RANKL-mediated osteoclastogenesis by RAW 267.4 cells. **A**. Western blot analysis (left) of OPG and RANKL secreted by mMSCs exposed to different scaffolds (CS, SCS, CCS or BCS). Expression levels of OPG, RANKL and OPG/RANKL ratio of the different groups were normalized against β–actin. For each parameter, groups identified with the same upper case letters, lower case letters or numbers are not significantly different ($P > 0.05$). **B**. Representative images of TRAP-stained osteoclasts and resorption pits produced by RAW 267.4 cells co-cultured with scaffold-

conditioned osteoblasts in the presence of RANKL (50 ng/mL; magnification 40×). The inhibition effect produced by anti-OPG antibody is shown on the far-right. **C** and **D**. Bar charts depicting the number of TRAP-positive multinucleated cells (10 fields) and area of resorption pits. For each chart, groups identified with the same upper case letter are not significantly different ($P > 0.05$).

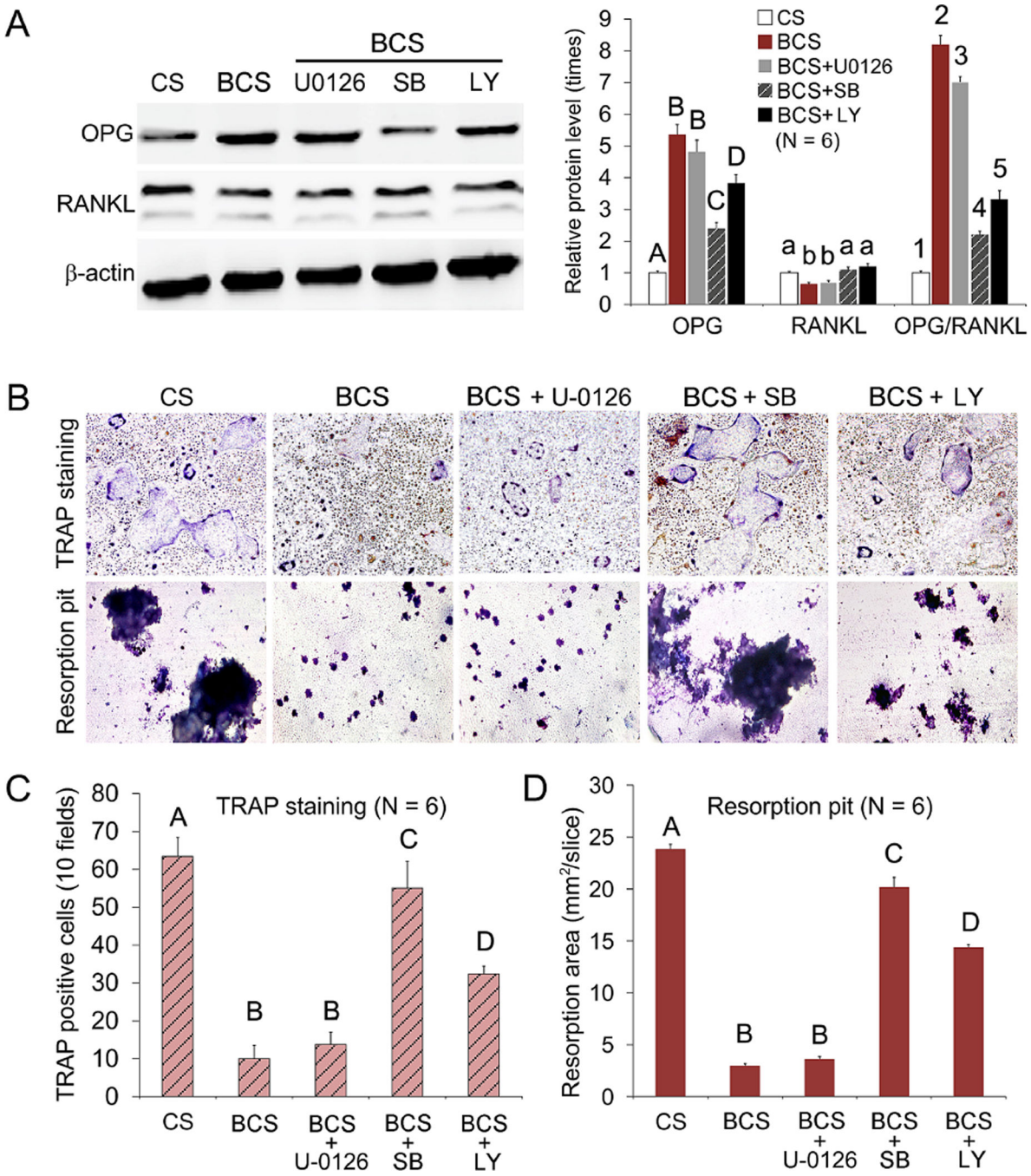

Figure 5.

A. Western blot of OPG and RANKL secreted by mMSCs exposed to BCS before and after the mMSCs were pre-treated with U0126, SB203580 (SB) or LY294002 (LY), inhibitors for the ERK, p38 and Akt signaling pathways, respectively. mMSCs cultured with collagen scaffolds (CS) were used as the negative control. For each parameter (OPG, RANKL, OPG/RANKL ratio), groups identified with the same upper case letters, lower case letters or numbers are not significantly different ($P > 0.05$). **B**. Representative images of TRAP-stained osteoclasts and resorption pit produced by RAW 267.4 cells co-cultured with BCS

before and after the addition of U0126, SB203580 (SB) and LY294002 (LY) pathway inhibitors (magnification 40×). **C** and **D**. Bar charts depicting the number of TRAP-positive multinucleated cells (C; 10 fields) and area of resorption pits (D). For each chart, groups identified with the same upper case letter are not significantly different ($P > 0.05$).